TUNABLE SiGe DETECTORS

CALSPAN - UB Research Center

Jorge R. Jimenez

19960924 060

This report has been reviewed by the Rome Laboratory Public Affairs Office (PA) and is releasable to the National Technical Information Service (NTIS). At NTIS it will be releasable to the general public, including foreign nations.
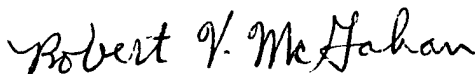
RL-TR-96-140 has been reviewed and is approved for publication.

APPROVED:

DARIN J. LEAHY
Project Engineer

FOR THE COMMANDER:

ROBERT V. MCGAHAN
Acting Director
Electromagnetics & Reliability Directorate

REPORT DOCUMENTATION PAGE

Form Approved
OMB No. 0704-0188

1. AGENCY USE ONLY (Leave Blank)	2. REPORT DATE	3. REPORT TYPE AND DATES COVERED
	August 1996	Final Oct 95 - Oct 96

4. TITLE AND SUBTITLE

TUNABLE SiGe DETECTORS

5. FUNDING NUMBERS

C - F30602-93-D-0075,
        Task 16
PE - 61102F
PR - 2305
TA - C1
WU - P3

6. AUTHOR(S)

Jorge R. Jimenez

7. PERFORMING ORGANIZATION NAME(S) AND ADDRESS(ES)

CALSPAN - UB Research Center
P.O. Box 400
Buffalo NY 14225

8. PERFORMING ORGANIZATION REPORT NUMBER

N/A

9. SPONSORING/MONITORING AGENCY NAME(S) AND ADDRESS(ES)

Rome Laboratory/EROI
80 Scott Drive
Hanscom AFB MA 01731-2909

10. SPONSORING/MONITORING AGENCY REPORT NUMBER

RL-TR-96-140

11. SUPPLEMENTARY NOTES

Rome Laboratory Project Engineer: Darin J. Leahy/EROI/(617) 377-5184

12a. DISTRIBUTION/AVAILABILITY STATEMENT

Approved for public release; distribution unlimited.

12b. DISTRIBUTION CODE

13. ABSTRACT (Maximum 200 words)

The theory of voltage-tunable cut-off wavelength silicide/SiGe/Si detectors is presented. Experimental data on tunable PtSi/SiGe/Si detectors is also presented. The theory is able to account for the experimentally observed behavior of tunable PtSi/SiGe/Si diodes. The tunability provided by the SiGe layer is understood as being due to two related effects: first, keeping the barrier peak position fixed with bias; and second, moving the barrier peak further away from the interface. The second effect decreases quantum efficiency, which depends on the peak-to-interface distance. However, maximizing the first effect allows us to obtain desired levels of tunability without potential decreases in quantum efficiency. For voltage-switched, dual-window imaging, a tunable range of 5-12μm is required over moderate voltages (10-15 volts), for which calculated detector parameters are Ge percentages of at least 20%, and total SiGe thicknesses (uniform plus graded) of $\sim$ 60-100 A and boron doping levels of $\sim$ 4-8 x 10^{16} cm^{-3} throughout the depletion layer width ($\sim$ 4000 A, in the SiGe and in the underlying Si).

14. SUBJECT TERMS

Tunable silicon germanium infrared detectors

15. NUMBER OF PAGES
36

16. PRICE CODE

17. SECURITY CLASSIFICATION OF REPORT	18. SECURITY CLASSIFICATION OF THIS PAGE	19. SECURITY CLASSIFICATION OF ABSTRACT	20. LIMITATION OF ABSTRACT
UNCLASSIFIED	UNCLASSIFIED	UNCLASSIFIED	UL

TABLE OF CONTENTS

Abstract

In this report, the theory of voltage-tunable cut-off wavelength silicide/SiGe/Si detectors is presented. Experimental data on tunable PtSi/SiGe/Si detectors is also presented. The theory is able to account for the experimentally observed behavior of tunable PtSi/SiGe/Si diodes. The tunability provided by the SiGe layer is understood as being due to two related effects: first, keeping the barrier peak position fixed with bias, and second, moving the barrier peak further away from the interface. The second effect decreases quantum efficiency, which depends on the peak-to-interface distance. However, maximizing the first effect allows us to obtain desired levels of tunability without potential decreases in quantum efficiency. For voltage-switched, dual-window imaging, a tunable range of 5-12 μm is required over moderate voltages (10-15 volts), for which calculated detector parameters are Ge percentages of at least 20%, total SiGe thicknesses (uniform plus graded) of ~ 60-100 Å and boron doping levels of ~ 4-8 x 10^{16} cm^{-3} throughout the depletion layer width (~ 4000 Å, in the SiGe and in the underlying Si).

Introduction

The advantages of PtSi arrays, (low cost, monolithic integration with Si readout circuitry, and excellent uniformity) have led to the search for silicide systems, or silicide-like Si-based systems, that can also do imaging at the long wavelength window of 8-12 μm.[1] This requires silicide barrier heights of ~ 0.10-0.12 eV, which have been achieved by IrSi/Si,[2] SiGe/Si heterojunction internal photoemission (HIP) detectors,[3] spike-doped PtSi/Si,[4] and PtSi/SiGe detectors.[5] SiGe layers, however, can also provide an additional enhancement to PtSi detector technology, that of voltage-tunable cut-off wavelengths. Such voltage tunable detectors would enable one to obtain and compare spectral information over the two atmospheric windows by the simple procedure of varying the applied bias. Other detector structures described as tunable have also been recently reported, such as Ir/Si/ErSi$_2$ and Cr/Si/SiGe (p+) TIPS (tunable internal photoemission sensors),[6] and Si homojunction interfacial workfunction internal photoemission (HIWIP) detectors.[7] HIWIPs are designed for the far infrared (40 μm and greater) and the tunable structures described here have the advantage over TIPS of not requiring the overgrowth of Si on a metal layer.

This report describes the theory of tunable PtSi/SiGe/Si detectors. The complete set of experimental data on tunable PtSi/SiGe/Si detectors is also documented, which this theory is able to model quite well.

I. Band diagram of metal/SiGe/Si Schottky diodes

In this section we calculate the band diagram for a metal-semiconductor junction in close proximity to a semiconductor-semiconductor heterojunction. The starting point is the built-in potential qV_{bi} , from which the depletion-layer width, $W(V,V_{bi})$, and the electrostatic potential energy in the depletion region, $U(z,W)$, are calculated. Figure 1 and Figure 2 shows the textbook situation for a Schottky diode. (Hole energies are increasing upward in all diagrams in this paper.) In Figure 1, the charges are not yet allowed to move or to come to equilibrium, and the built-in potential difference is the difference between the Fermi levels.
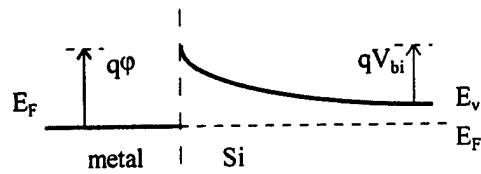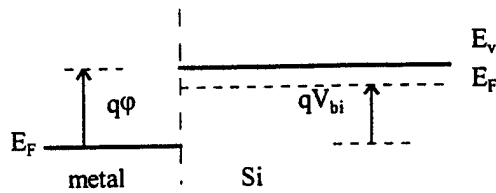

Figure 1 Metal/Si interface, with bands lined up, but without charge flow. The difference between Fermi levels is qV_{bi} .

Figure 2 Metal/Si interface after charge flow; qV_{bi} is the shift in the valence band between the bulk and the interface.

Similarly, Figure 3 shows the bands of a metal, a thin SiGe layer, and a Si substrate, not yet allowed to come to equilibrium, where the metal and SiGe bands are separated by the metal/SiGe Schottky barrier height and the SiGe and Si bands are separated by empirically determined offsets. If the SiGe layer is thin enough, charge will flow from both the SiGe layer and the Si substrate to the metal, producing the bands shown in Figure 4. In this diagram there is no simple visual analog to value of qV_{bi} , as in Figure 2. Rather, the built-in potential of a metal/SiGe/Si diode is the difference in Figure 3 between the metal Fermi level and the Si Fermi level, i.e.,

$$qV'_{bi} = q\phi^x_{bo} + \Delta E^x_v - [E_F - E^\infty_v] \qquad\qquad 1$$
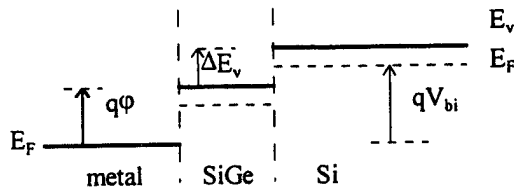

Figure 3 Metal/SiGe/Si band alignments (no charge flow) determined by the experimental values of the Schottky barrier height and the valence band offset.
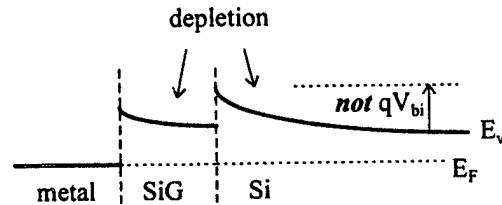
Figure 4 Metal/SiGe/Si bands in equilibrium. Both SiGe and Si are depleted as charge flows from both to the metal.

2

where $\Delta E_v{}^x$ is the SiGe/Si band offset, x is the Ge percentage in the SiGe alloy, $\phi_{bo}{}^x$ is the asymptotic[8] value of the intimate metal/$Si_{1-x}Ge_x$ Schottky barrier, and E^∞_v is the valence band-edge energy in the neutral region of the semiconductor. Since the values of intimate PtSi/SiGe diodes are still unmeasured, we assume for calculational purposes in this paper asymptotic barrier heights of 0.22, 0.20, and 0.18, and 0.16 eV for 5, 10, 15, and 20% Ge, respectively (compared to an asymptotic barrier height of 0.24 eV for PtSi/Si). This does not detract from the generality of the results about the tunable behavior of silicide/SiGe/Si diodes.

The depletion region width $W(V,V_{bi})$ is obtained in the usual manner[9] by from equation (2). Because of the addition of the SiGe/Si offset to this equation, the depletion width of silicide/SiGe/Si diodes is somewhat larger than that of the corresponding silicide/Si diode, assuming the silicide/SiGe barrier height is reduced compared to the silicide/Si barrier height by less than the SiGe/Si offset.

$$W(V) = \sqrt{\frac{2\varepsilon}{qN_a}\left[V_{bi} + V + \frac{kT}{q}\right]} \qquad\qquad 2$$

The electrostatic potential energy U(z,V) due to the space charge in the depletion region is

$$U(z,V) = \frac{q^2 N_a}{\varepsilon}\left[W(V)z - \frac{z^2}{2}\right] \qquad\qquad 3$$

where N_a is the doping in the SiGe and Si, ε is the dielectric constant of Si, T is the absolute temperature, k is Boltzmann's constant, V is the externally applied bias, and z is the distance from the metal-semiconductor interface. (Equation (3), derived by an integration through the depletion region, can be used assuming a constant dielectric constant approximation. This is a good approximation given the dielectric constants of ~ 12 for Si, 16 for Ge, Ge concentrations of only 20-30 %, and SiGe thicknesses less than 1% of the depletion region thickness.)

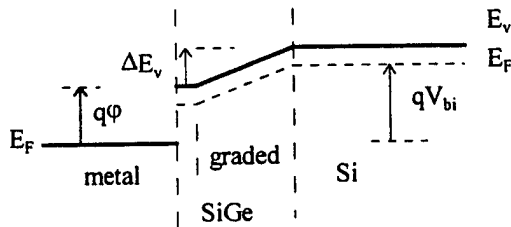The potential energy is referred to a zero of energy at the metal Fermi level, and the valence

Figure 5 Non-equilibrium diagram showing Metal/SiGe/Si band alignments determined by the experimental values of the Schottky barrier height and the valence band offset
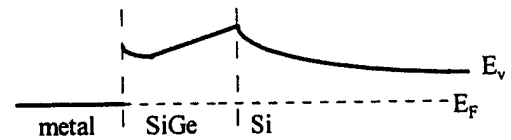
Figure 6 Metal/SiGe/Si bands in equilibrium. Both SiGe and Si are depleted charge flows from both to the metal.
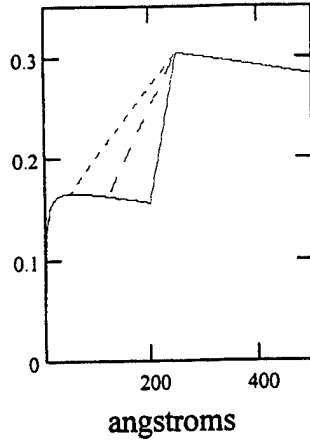
3

Figure 7 Calculated valence band diagrams with varying SiGe graded layer thicknesses but constant total thickness.
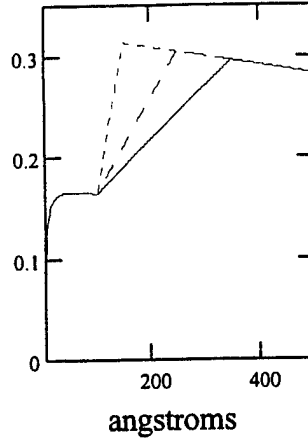
Figure 8 Calculated valence band diagrams with varying SiGe graded layer and total thicknesses.
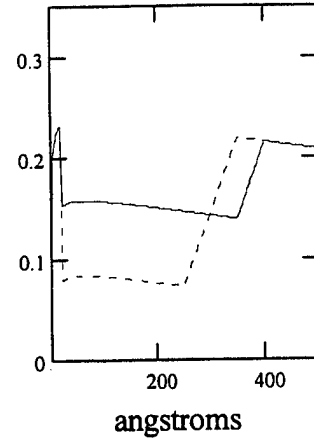
Figure 9 Calculated valence band diagrams with residual Si layer determining barrier height at the interface.

band-edge energy, $E_v(z)$, is obtained from the electrostatic potential energy by

$$E_v(z,V) = E_v^i(z) + U'(z,V) + \frac{q^2}{16\pi\varepsilon_s z} \qquad 4$$

where $E_v^i(z)$ is the initial valence band energy diagram, as for example in Figure 3, or in Figure 5, where part of the SiGe layer is graded. Adding the electrostatic potential energy $U(z,V)$ to the initial profile $E_v^i(z)$ results in the bent-band diagram as shown, for example, in Figure 6. It will be noted that the height of the SiGe/Si interface peak is the same whether or not the SiGe is graded (Figures 7,8). This allows us to tailor the grading profile to optimize diode properties independently of the desired Ge concentration. Note that, depending on the value of the intimate PtSi/SiGe barrier height, the total barrier height in intimate diodes (including the SiGe/Si offset peak) can be higher than the PtSi/Si barrier height.

II. Fabrication of silicide/SiGe interfaces

An important parameter in the band diagrams of silicide/SiGe/Si diodes is the value of the silicide/SiGe barrier height. Schottky diodes can be formed on SiGe by the reaction of a deposited metal film on a SiGe layer, producing a potentially complicated mixture of silicides, germanides, germano-silicides, Si, Ge, and SiGe of modified stoichiometry and crystallinity. In the case of Pt on SiGe, it has been reported that the preferred phase to form is PtSi, resulting in Ge segregation and/or a Ge-rich layer at the interface. However, published results in the literature do not agree on the values of the barrier heights of diodes made involving Pt-SiGe reactions. For example, Kanaya et al.[10] reported barrier heights that were lower than PtSi/Si, while Liou et al.[11] and Xiao et al.[12] reported barrier heights that were higher than PtSi. The most recent experiments on Pt-SiGe

reacted diodes give varying results for the barrier heights, when varying fabrication and deposition conditions are involved.[13]

While this situation has not yet been clarified, other ways have been used to fabricate silicide/SiGe system that avoid the complications of metal-SiGe reactions. One method is to grow a Si capping layer of appropriate thickness on the SiGe, with which a deposited Pt layer also of appropriate thickness would then react.[12] If the thicknesses are such that the Si layer is not totally consumed by the Pt, then a very thin layer of Si will remain. The band diagram would then look like Figure 9, where a thin Si "barrier" is produced by the unconsumed Si. (Image force lowering does not remove this effect.) Thus the "barrier height" (i.e., the alignment of bands) at the interface is still that of PtSi/Si, but carriers can tunnel through the Si "barrier", and the

Figure 10   Calculated variation of the PtSi/Si barrier height with reverse bias for 10^{15} cm^{-3}, 10^{16} cm^{-3}, and 10^{17} cm^{-3} doping levels.

effective, or observed, barrier height will be reduced.[14]   The effects of the offset at the second SiGe/Si offset can be removed, if desired, by inserting a graded SiGe layer to smooth away the offset. If not, the important point to be observed is that the total barrier height can never exceed the PtSi/Si barrier height. For this band diagram, the equations are those of a normal PtSi/Si Schottky band diagram, where qV_{bi} reverts back to its normal Si value, the depletion widths are the same as PtSi/Si, and the only difference from a PtSi/Si diagram is a segment that is offset downward by the SiGe.

The second method is to simultaneously deposit Pt and Si in the correct (stoichiometric) ratio on SiGe. For diodes made by the second method (stoichiometric codeposition), the PtSi and SiGe are in intimate contact.   The intimate PtSi/SiGe barrier height cannot be deduced from the barrier height of PtSi/SiGe diodes made from the Si cap because of the different interface mechanisms (such as interface chemistry, bonding, and states) that come into play.   However, experiments on intimate PtSi/SiGeC diodes made by codeposition have resulted in barrier heights that are lower than PtSi/Si.[15] This result may be taken as an indication that the intimate PtSi/SiGe barrier height will be lower than the PtSi/Si barrier height.

III. Voltage-dependence of Silicide/SiGe/Si diodes: Tunable detectors

The barrier heights of Schottky diodes have only limited bias dependence. They vary only as the fourth root of the voltage:

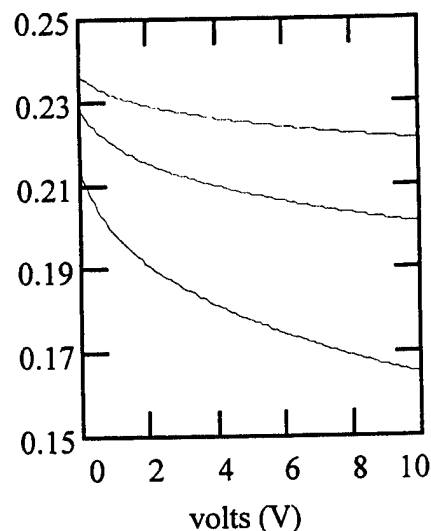$$\varphi(V) = \varphi_o - \frac{q}{2\varepsilon_s}\sqrt{\frac{NW}{\pi}} \qquad\qquad 5$$

where W is the depletion width in equation (2). Figure 10 shows the variation of the PtSi/Si Schottky barrier height with reverse bias for different doping levels. Higher doping levels result in increased variability. However, the increased doping by itself is not a viable way of making tunable detectors because higher doping levels result in increased tunneling and higher dark currents. Furthermore, the tunability obtained from increased doping, although substantial (e.g. 5.7 μm - 7.5 μm over 0-10 volts for 10^{17}cm^{-3} doping) is not enough, because tunable detectors will not become attractive for infrared imaging applications unless they can be tuned all the way from 5 to 12 μm.

That the Schottky barrier height depends on reverse bias is due entirely to the image force. The image force modifies the electrostatic potential due to the space-charge (depleted) region, which has its maximum right at the metal-semiconductor interface. Adding the image potential to this electrostatic potential forms a barrier with its maximum inside the semiconductor, a short distance (60-20 Å, depending on doping) away from the metal. When a reverse bias is applied, this maximum is lowered, but is also shifted closer to the metal-semiconductor interface, because of the shape of the Schottky barrier. Figure 11 shows Schottky barriers calculated for two doping concentrations, 10^{15}cm^{-3} and 10^{17}cm^{-3}, each at zero and ten volts bias. The position of the maxima for each of these curves is marked, and also for intermediate biases between 0 and 10 volts (1 volt increments), so that the dependence of the barrier height and its position on bias is clearly visualized. It will be noted that the energy shift of the barrier maximum is much greater for the

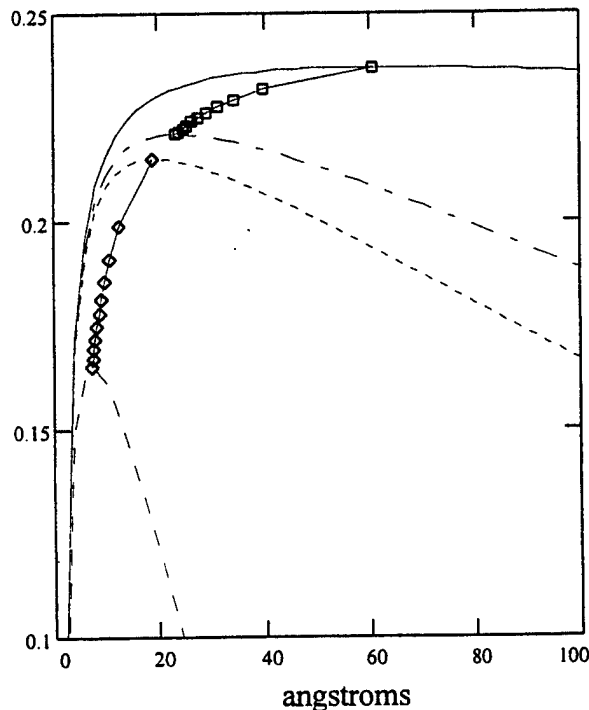Figure 11: PtSi/Si Schottky barrier bands calculated at 1 and 10 volts reverse bias for 10^{15} cm^{-3} and 10^{17} cm^{-3} doping, with the barrier maxima marked at 1 volt intervals.
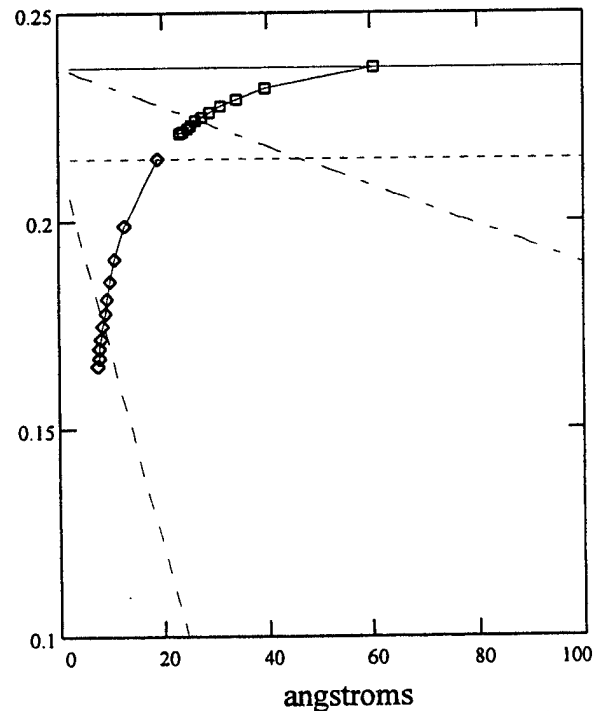
Figure 12 Reverse bias potentials, for 10^{15} cm^{-3} and 10^{17} cm^{-3} doping. Horizontal lines are the zero volt references and sloping lines represent the change in potential energy at 10 volts.
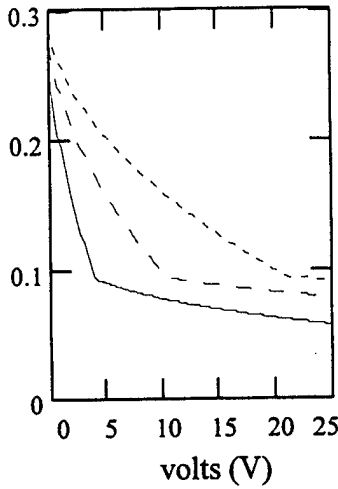
6

Figure 13 Tunable barrier heights for different doping concentrations (2, 4, and 10 10^{16}cm^{-3}), 60 A Si$_{0.8}$Ge$_{0.2}$, assuming an asymptotic PtSi/SiGe barrier height of 0.16 eV. highly doped (10^{17}cm^{-3}) diode.
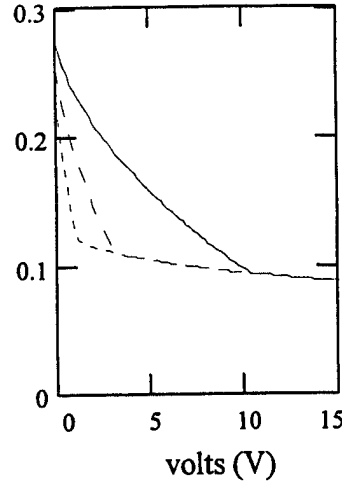
Figure 14 Tunable barrier heights for different Si$_{0.8}$Ge$_{0.2}$ thicknesses (60, 100, and 150 A) 4x10^{16}cm^{-3} doping, assuming an asymptotic PtSi/SiGe barrier height of 0.16 eV.
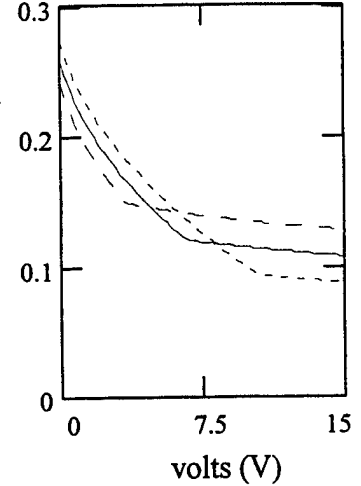
Figure 15 Tunable barrier heights for 10, 15, and 20% Ge (4x10^{16}cm^{-3} doping, 60 A) assuming asymptotic PtSi/SiGe barrier heights of .20, .18, and .16 eV.

Figure 11 suggests that another way to obtain increased tunability would be to change the shape of the Schottky barrier in such a way that the peak did not shift closer to the interface with increasing bias. In Figure 12 the change in the potential energy due to the externally applied bias is shown, a straight line extending downward through the depletion region. The slope of the line is zero at zero bias, and increases in magnitude with increasing bias. Figure 12 shows the calculated potential energy changes due to the reverse bias (10 volts) for the profiles shown in Figure 11. The origins are positioned so that the zero slope lines coincide with the Schottky barrier maximum at zero bias. The potential energy for all biases must coincide at the metal-semiconductor interface. By examining this figure, it can be readily seen that if the Schottky barrier maximum did not change in position with bias, the change in barrier height (corresponding to the vertical displacement between the two straight lines at the zero-bias position) would be greater. Since the position of the peak does not shift with bias, the change in the barrier height with voltage is simply the change in the electrostatic potential energy U(z,V), represented by equation (3), calculated at a given position z_{int}. This gives (equation 6)

$$\Delta \phi_{eff} = -\frac{q}{\varepsilon_s} N_a [W(V) - W(V = 0)]_{z_{int}} \qquad 6$$

Thus the barrier height change depends directly on the SiGe thickness z_{int}, and varies linearly with W, in contrast to equation (5), which depends on the square root of W, and therefore on the fourth root of V. This change from the fourth root to the square root is due entirely to keeping the peak position fixed with position as the bias varies.

7

The barrier height itself, as a function of bias can be obtained as follows: For reverse biases such that the valence band at the SiGe/Si interface is of greater energy than the valence band at the Schottky barrier peak position, the effective barrier height, ϕ_{eff}, is simply the value of the valence band energy at the SiGe/Si interface, referred to the metal Fermi energy, as expressed in equation (7)

$$-q\,\phi_{eff} = E_v(z_{int}) \qquad\qquad 7$$

Writing this out explicitly gives equation (8)

$$q\,\phi_{eff} = -U(z_{int},W'(V,V'_{bi}(\phi^x_{bo},\Delta E^x_v))) + \frac{q^2}{16\pi\varepsilon\,z_{int}} + q\,\phi^x_{bo} + \Delta E^x_v \qquad\qquad 8$$

where U is the electrostatic potential energy as given in equation (3) and W is as given in equation (2). It must be emphasized that equation (8) refers to the barrier maxima of valence band diagrams, as distinct from barrier heights extracted from some measurement technique, which will be dealt with later. For reverse biases such that the SiGe/Si peak offset is lower than the Schottky barrier, the effective barrier height is that of the normal Schottky diode. Thus the enhanced tunability holds only for biases smaller than a certain critical bias, at which the SiGe/Si barrier moves below the PtSi/SiGe barrier. A plot of the barrier maxima versus bias will therefore look like the curves in Figures 13, 14, and 15, calculated for different SiGe thicknesses and doping concentrations.

In Figures 13,14, and 15 we see that the tunable range of barrier heights is set primarily by the Ge concentration, and also secondarily by the SiGe thickness. The thickness and doping primarily determine the sensitivity of the barrier heights to the applied bias, i.e., the tunable voltage domain. Increasing the thickness also reduces the range of barrier heights somewhat because of the curvature of the depletion region. Since the quantum efficiency of detectors depends on the peak-to-interface distance, there is a trade-off between increased sensitivity and the quantum efficiency of the detectors. Design of optimum tunability therefore requires consideration of the dependence of the quantum efficiency on SiGe thickness.

IV. Quantum Efficiency Coefficient C_1 of Tunable Detectors

The internal quantum efficiency (quantum efficiency per absorbed photon) of silicide infrared detectors is given by the modified Fowler equation,[16]

$$Y = C_1\frac{(hv - \varphi)^2}{hv} \qquad\qquad 9$$

where the coefficient C_1, obtainable from the slope of the Fowler plot, has been called the Schottky emission coefficient, but is perhaps more descriptively called the quantum efficiency coefficient. The quantum efficiency coefficient C_1 increases with bias, and has been found to have a bias dependence of the form[17]

$$C_1 = C_0 \exp(-z_m(V)/L) \qquad \qquad \textbf{10}$$

where $z_m(V)$ is the distance from the Schottky barrier peak to the metal-semiconductor interface, L is a composite scattering length, and C_0 is a constant. The peak distance z_m is given by

$$z_m^2(V) = \frac{1}{16\pi N W(V)} \qquad \qquad \textbf{11}$$

where W(V) is the depletion layer width given in equation (2).

For tunable detectors, we expect that C_1 follows this behavior only at higher biases where the SiGe/Si barrier is lower than the Schottky barrier. For lower biases corresponding to emission over the SiGe/Si bias, we expect that C_1 will have no variation, because the SiGe/Si peak position does not shift with bias. This behavior of C_1 can be considered a key signature of tunable emission over the SiGe/Si barrier, as distinguished from other bias-dependent mechanisms, such as heavy doping. (This will be true to the extent that C_1 depends only on the peak position and not on other bias-related factors.) Data showing this type of behavior is presented later.

V. Parameters for tunable infrared detectors

By tunability, we mean both a range of tunable barrier heights and a voltage domain over which those barrier heights are obtained. Obtaining practical levels of tunability means adjusting both The barrier height range is essentially determined primarily by the SiGe/Si offset value, or the SiGe composition, and only secondarily by the SiGe thickness and doping. The tunable voltage domain is determined primarily by the SiGe thickness and doping, and secondarily by the SiGe composition. (See Figures 13-15.) Voltage-tunable detectors, in order to be attractive for infrared imaging applications, must be able to switch from cut-offs of 5 μm, or less, to cut-offs of 12 μm. This translates to barrier heights of 0.1 eV to about 0.22 eV (or higher, if the 3-5 μm window is required to be switched out as well), a tunable range of at least 0.12 eV. This implies a Ge percentage of about 20%. For practical reasons, the full range of barrier heights should be attainable with moderate voltage domains of 0-10 or 0-15 volts. However, keeping the present levels of quantum efficiency implies keeping the SiGe/Si interface distance approximately the same as the present PtSi/Si Schottky-diode maximum of about 60 Å (60 Å at 10^{15} cm^{-3} doping). Given this thickness constraint, the desired voltage domain can be obtained by increasing the doping level. However, the doping levels should not be too high to avoid increased substrate absorption and tunneling. Fortunately, the doping levels need to be increased only in a layer of the same thickness as the expected zero-voltage depletion width. (Thicknesses greater than this will do nothing to

9

increase the tunability.) Calculations (Figures 13-15) show that for the desired tunable domain can be attained by doping levels of less than 10^{17} cm^{-3}. The theoretical optimum configuration, a good starting point for experiments, is a SiGe thickness of 60 Å, and a doping level of 4×10^{16} cm^{-3} in the SiGe and in 4000 Å of Si below the SiGe. The tunable barrier height range is determined by the Ge percentage through known SiGe/Si offsets, but the value of the low-barrier end of the range is set by the Ge percentage through as-yet unknown PtSi/SiGe intimate barrier heights. These detector parameters have been calculated using an estimated asymptotic barrier height of 0.16 eV for 20% Ge. This may be increased if the intimate barrier heights have a weaker dependence on Ge concentration. This will also serve to increase the high-barrier end of the range, which is not critical because it can be lowered by the proper operating bias.

Figure 18 shows the calculated band diagrams for a PtSi/SiGe/Si diode (linearly graded with 20% Ge content at the surface) at two doping levels: 10^{15} cm^{-3} at 0 and 10 volts reverse bias, and 4×10^{16} cm^{-3} at 0 and 10 volts reverse bias. The thickness of the SiGe layer is such that its interface peak (the SiGe/Si interface) coincides with the PtSi/Si Schottky barrier maximum at zero volts (60 Å). The more "pointed" nature of the peak, which might result in increased tunneling current, can be reduced by engineering the grading profile to make it more "rounded". However, this must be done carefully to ensure that the peak remains fixed with position. The use of graded Ge profiles, instead of abrupt interfaces, also serves to avoid double peak structures which might result in anomalous resonant-tunneling effects.

Figure 16 Calculated valence band diagrams of a PtSi/SiGe/Si diode at 4×10^{16} cm^{-3} with 0 and 10 volts reverse bias, and a PtSi/Si diode at 10^{15} cm^{-3} with 0 and 10 volts reverse bias, again assuming an asymptotic value of 0.16 eV for the PtSi/SiGe intimate barrier height.

VI. Barrier heights obtained from photoresponse measurements

The barrier heights we have been discussing so far are the theoretical values of the barrier maxima. For silicide/SiGe/Si diodes, some care is required in interpreting the barrier heights derived from photoresponse measurements. This is because for diodes in which the SiGe/Si offset peak is far away from the interface (compared to the usual distance of 60 Å for PtSi/Si diodes), not only is the probability of carriers' making it over the barrier reduced (which results in reduction in C_1), but a greater fraction of carriers that do make it over the barrier will suffer energy losses. The expected effect of such energy losses would be to raise the "apparent" barrier height extrapolated from photoresponse measurements. This can be better understood by considering only that fraction of emitted carriers that start out from the metal-semiconductor interface towards the barrier maximum, suffer some phonon collisions that cause it to lose some energy, and end up at the barrier maximum with the right momentum direction to be emitted. At a photon energy equal to
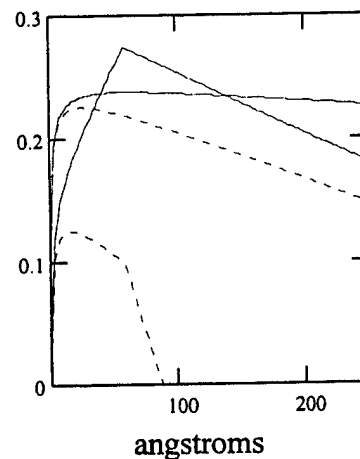
10

the Schottky barrier height, no carriers of this type will be emitted because they do not have enough energy. As the photon energy increases, the fraction of carriers of this type that will be emitted will increase, resulting in a C_1 value that increases with energy, and therefore gives some upward curvature (a roll-on) to the Fowler plot. At some higher energy where all carriers of this type arrive at the interface with the right amount of energy for emission, the C_1 ceases to change, and the Fowler plot starts its linear behavior. The barrier heights obtained by extrapolating the linear part of the Fowler plot will therefore be higher than the actual height of the barrier peak. As the interface-to-peak distance in PtSi/SiGe becomes large (e.g. several hundred angstroms) the discrepancy will increase, and for such large distances the roll-on span a larger energy range, but will be smaller in magnitude. This may make it difficult to measure near the actual barrier height, and only that portion of the deviation near the linear part may be observed.

This effect is similar to that modeled by Mooney,[16] except that Mooney considered energy losses due to electron-phonon collisions in the *metal* before arriving at the metal-semiconductor interface, at which point they were assumed (neglecting carrier-scattering in the region between the metal-semiconductor interface and the Schottky barrier maximum) to be either emitted or not. The effect is different in that carriers in the metal are created throughout its width, while carriers in the semiconductor must all cross the image-force well starting from one side. The Vickers-Mooney model was able to account for (among other things) the slight upward curvature in the Fowler plot typically observed in careful measurements of high-quality PtSi/Si diodes optimized for detector applications. Carrier scattering in the semiconductor region was treated later for its effect on C_1, but not on the barrier height or the shape of the Fowler plot. For the metal-to-peak distances involved in typical PtSi detectors this effect may be small, or negligible, and no unexplained observations have demanded that the energy losses due to scattering in the semiconductor be treated. Recent ballistic electron emission microscopy (BEEM) studies[18] have treated the effects of scattering in the semiconductor on transmission probabilities, i.e., on the BEEM current. For PtSi/SiGe detectors in which the SiGe becomes very large, such as those previously reported, the effects of the energy losses due to scattering in the semiconductor may become quite pronounced. For such cases, a more complete treatment, taking into account energy losses due to scattering processes in both the metal and in the semiconductor before the barrier maximum, would seem to be appropriate.

VII. Data

Updated and refitted data on the following samples are documented in this report. The refitting was done for better consistency between plots taken at a varying biases. They were also done in a way more consistent with theory. For example, for lower biases in the tunable range, it is more appropriate to fit the higher energy part.

The samples are a series (STRM1-5) of PtSi/SiGe/Si diodes of varying SiGe concentrations (5,10,15,20%) and thicknesses. The SiGe was grown by RTCVD (rapid thermal chemical vapor deposition) by the Princeton group of Prof. James C. Sturm. A 40-Å Si cap was grown on the SiGe. The SiGe was not intentionally doped, and hence the true doping is unknown. The

11

thicknesses of the graded-Ge portions are uncertain, because of the nonlinear dependence of the growth rate on germane flow rate. Sample thicknesses estimated from growth conditions are 500-600 Å for the 20% sample and 700-800 Å for the 15% sample. These and other SiGe sample parameters have been previously documented.[19] Pt was deposited in a system at the David Sarnoff Research Center.

Figure 17 shows the calculated valence band diagrams for the 20 and 15% samples using the SiGe thicknesses known from growth conditions. The bands are calculated for two doping levels: 10^{15} cm^{-3} and 10^{16} cm^{-3}. The diagrams are drawn presuming that some unreacted Si remains between the PtSi and the SiGe. Note that, if this presumption is true, the total height of any point in the band cannot exceed the PtSi/Si barrier height. The doping level has a profound effect on the height of the SiGe/Si offset peak. The thicknesses of the SiGe were verified with SIMS for the 20% Ge sample. The thicknesses are rather large, far from the theoretical optimum values from tunable detectors, because this was not the original purpose of the samples.
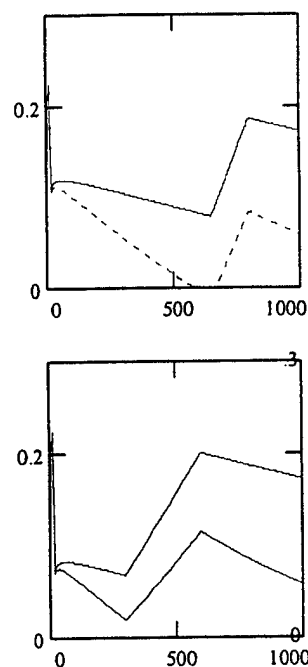
Figure 18 shows the photoresponse data for the 20% sample (STRM1) with the original linear fits. This plot and/or its derived barrier heights appears in SPIE and MRS conference proceedings[20,21]. Figure 19 shows the same photoresponse data with refitted Fowler plots. While this plot has not been published, its revised barrier heights have appeared in a journal publication.[5] The data were fitted with more consistency over the various biases. The revised barrier height and C_1 data are also shown in Figure 19. Note that the low-bias barrier heights have been shifted higher. It should be noted for the record that because these values have been refitted, they are different from the original data that appear in the Rome Lab data logbooks. Data for samples STRM2 - STRM5 have been documented in previous reports.[19]

After samples STRM1-STRM5 were measured, another set of samples were taken from the same wafer and annealed in forming gas. This was done to see whether the excess tunability was more of an artifact than a permanent effect. These samples were denoted STRM6-STRM10. There was no significant change in their tunable behavior. The photoresponse data for sample STRM6 is shown in Figure 20. The fits of this plot are also revised from the original fits in Rome Lab data logbooks.

In the same way, Figures 21 and 22 show the photoresponse data with refitted Fowler plots for the 15% Ge sample (STRM7). Figure 22 was used in a recent journal publication.[5] No refits have been done on the 10% and 5% samples, as these show normal tunability and the fitting is less crucial to the interpretation of barrier height data. Figure 23 shows the photoresponse data for the 10% Ge sample (STRM8). This was used in a conference proceeding and has also been documented in a previous report.[19] Figure 24 shows the photoresponse data for the 5% sample

Figure 17 Calculated valence band diagrams for 20% and 15% Ge samples.

(STRM9). This has not been previously published or documented in a report. STRM10 was a control sample that used a Si wafer with no epi growth. Its Fowler plots have been previously documented.

VIII. Fitting the model to the measured barrier heights

Fitting the theoretical model described in the previous section to the present data is complicated by effects of the parasitic Si barrier due to the unconsumed Si, if present. At high biases beyond the onset of saturation, the tunneling will cause the saturation value of the extrapolated barrier height to be higher than it actually is. At zero bias, this will have no effect since carriers must be have energy at least as high as the Si barrier in order make it over the SiGe/Si offset. At intermediate biases before the onset of saturation, an effect increasing with bias would be expected, changing the observed bias-dependence of the extrapolated barrier heights.

The revised barrier heights of samples STRM1 and STRM7, together with the barrier heights of samples STRM8 and control sample STRM10, are shown in Figure 25. This Figure has been used in a recent publication.[5] Similar plots, but using the original (unrevised) barrier heights, were used in the conference proceedings.[20,21] The solid curves are fits using the theory described in previous sections, avoiding the complications of the parasitic Si barrier by assuming an intimate PtSi/SiGe interface. If this simplifying assumption is made, the intimate barrier height value is determined by the experimental saturation values. For the 20% Ge sample this between ~ 0.15-0.16 eV, and for the 15% Ge sample this is between ~ 0.19-0.20 eV. A range of acceptable doping values is also determined by the bias variation of the saturated barrier heights. The observed experimental variation of the saturation values indicate light doping, in the range of 10^{15} cm^{-3}. The effects of the energy losses due to scattering are included in an ad hoc manner by including an energy loss correction term ε_{loss}. (The theoretical basis for this has been described in section VI). It should be noted that many pairs of doping and thicknesses can reproduce the same tunable portion, because the slope, or curvature, of the tunable portion is proportional to both the thickness and the doping (equation 6). The following parameter sets are some of those that can give acceptable fits to the data.

20% Ge				15% Ge			
z_{sg} (Å)	ϕ_{asymp} (eV)	N_a (cm^{-3})	ε_{loss} (eV)	z_{sg} (Å)	ϕ_{asymp} (eV)	N_a (cm^{-3})	ε_{loss} (eV)
450	0.155	6.5 x 10^{15}	0.103	650	0.195	1.3 x 10^{16}	0.210
600	0.155	4.0 x 10^{15}	0.108	750	0.195	9.5 x 10^{15}	0.210
750	0.150	2.3 x 10^{15}	0.108	850	0.195	7.5 x 10^{15}	0.210

If the data are fitted by including the presence of a parasitic Si barrier due to an unconsumed Si layer, then the saturation value of the barrier height (defined as the height of the valence band at the normal Schottky barrier maximum) is not adjustable, but is simply the PtSi/Si barrier height reduced by the SiGe/Si offset. The offsets are calculated using the empirical formula for the
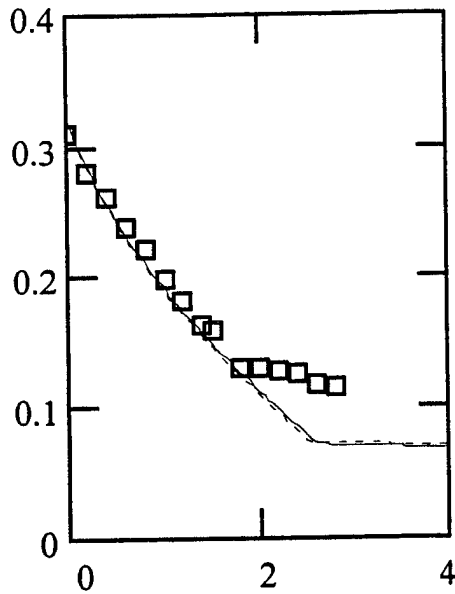
0.4

0.3

0.2

0.1

0

0   2   4

Figure 26 Theoretical curves fitted to the tunable part of the 20% Ge sample assuming unconsumed Si at the interface.
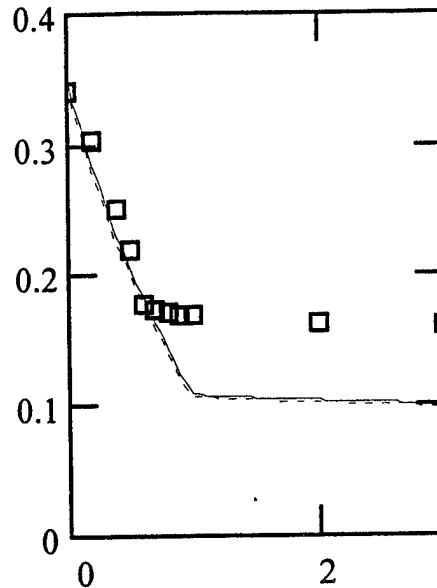
0.4

0.3

0.2

0.1

0

0   2

Figure 27 Theoretical curves fitted to the tunable part of the 15% Ge sample assuming unconsumed Si at the interface.

bandgap,[22] $\Delta E_g = 0.94x-0.43x^2+0.17x^3$, and a 9:1 division of the gap change between the valence and conduction bands. This gives a valence band offset ΔE_v of ~ 0.15 eV for 20% Ge and ~ 0.12 eV for 15% Ge. It is immediately noted that the experimental saturation values of the barrier heights are too high, given these offsets. However, the difference can be attributed to the barrier-raising effect of the parasitic barrier.[14] Figures 26 and 27 show a set of curves fitted to the tunable portion of the curve in this manner. The saturated part of the theoretical curve cannot be adjusted but is determined by the Ge percentage. Some parameter sets that can fit the data are:

20% Ge			15% Ge		
z_{sg} (Å)	N_a (cm^{-3})	ε_{loss} (eV)	z_{sg} (Å)	N_a (cm^{-3})	ε_{loss} (eV)
700	3×10^{15}	0.165	800	8×10^{15}	0.256
600	4×10^{15}	0.165	750	9×10^{15}	0.250

Figure 28 shows the C_1 data for the 10% sample together with a control Si sample. Figure 29 shows the C_1 data for the 15% and 20% sample, showing the expected drop. These plots are in the format used in the past, where $\ln(C_1)$ is plotted against the calculated peak position $z_m(V)$. The slope of the plot gives L and the linear extrapolation to z=0 gives C_0. Figures 28 and 29 together have appeared in a recent journal publication.[4] Similar plots usin the unrevised C_1's were used in the conference proceedings.[20,21] Figure 30 shows the effect of using different doping values to calculate the $z_m(V)$. A plot such as this is accurate for tunable detectors in the high-bias region, but in the low bias region, the values of z_m lose their meaning. For tunable detectors, therefore, a direct plot versus bias may be more appropriate. In order to see a change in behavior between standard diodes and tunable diodes, such a plot would preferably also be linearized, such as in Figure 31,
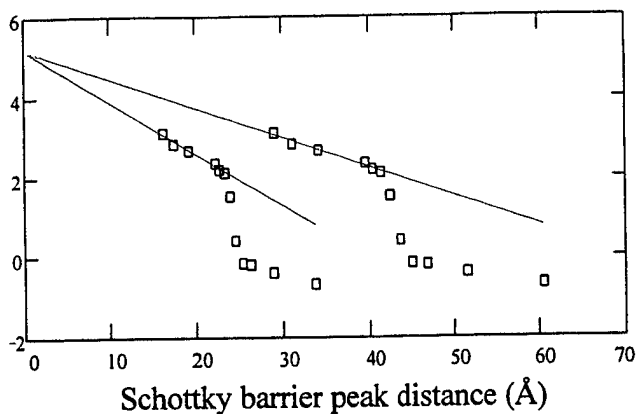
Figure 30 C_1 data from a tunable PtSi/SiGe/Si detector (taken from reference 5), plotted against Schottky barrier peak distances calculated for each bias using two different doping levels (10^{15} cm^{-3} and 10^{16} cm^{-3}). The linear portion corresponds to emission over the normal Schottky barrier and in both curves extrapolate to the same value of C_0 that can be used in a plot like Figure 17. The sharp drop in C_1 values corresponds to emission over the much further SiGe/Si peak offset but the z_m values of these data points are inappropriate.
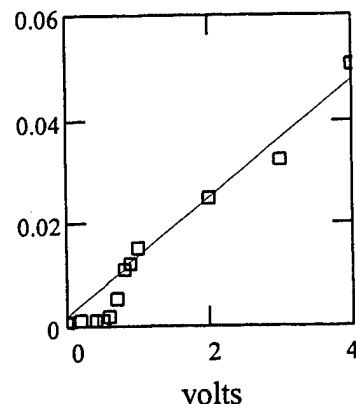
Figure 31 The same C_1 data as in Figure 16. The quantity $\ln^{-4}(C_0/C_1)$ is plotted directly against the bias voltage, where C_0 was obtained from Figure 16. The deviation from linearity corresponding to emission over the SiGe/Si barrier is smaller but still clearly evident.

where the quantity $\ln^{-4}(C_0/C_1)$ is plotted against bias. In order to be linear, however, this plot requires us to incorporate a previously extrapolated value for C_0, because of the singularity that occurs when $C \rightarrow C_0$.

If other bias-dependent mechanisms are considered, these mechanisms must also have the phenomenon of saturation. The mechanisms must also be consistent with the observed drop in C_1 at a bias that coincides with the shift from saturation to tunability. We can therefore eliminate other bias-dependent mechanisms such as heavy doping that cannot explain saturation or a C_1 drop. One possibility that remains is the phenomenon of pinch-off associated with Schottky barrier inhomogeneities, pointed out by Tung.[23] If the Schottky barrier varied along the plane of the interface on a length scale comparable to the depletion width, then at low biases, the regions of low barrier height are "pinched off" by the regions of higher barrier height, and a "saddle-point" barrier exists, further away from the interface than normal image-induced barrier maximum, with a value between the high and the low barrier height. As the bias increases the saddle-point barrier is lowered, the pinch-off is reduced, and eventually the regions of low barrier height are fully exposed. One can imagine the inhomogeneities to be caused by localized reactions of Pt with SiGe at some areas of the interface. The difference between this picture and that of tunable SiGe/Si offsets is that a mixture of barrier heights is always present. At low biases, we have a mixture of high and saddle-point barrier heights, and.at high biases, saturation occurs at a mixture of high and low barrier heights. Thus if there are two barrier heights we expect the high-bias Fowler plots to exhibit dual slopes, and if there is a mixture of barrier heights, perhaps a continuous curve to which no single slope can be fitted. The dual-slope, or many-slope Fowler plot should be observed at both low and high biases. More modeling of this effect is required to see if it can indeed account for the

15

data. It should be noted that, even if one assumes the picture of inhomogeneous barrier heights, the effects of the SiGe/Si offset must still be taken into account, and the band-diagram calculations do show that they should have observable effects. It should also be noted, however, that the idea of tunable SiGe/Si offsets can account for the observed data quite well, if one accepts the idea of carrier energy losses over distances of hundreds if angstroms.

The idea of "apparent" barrier heights from photoresponse that are shifted higher due to carrier energy losses during transport in the SiGe is not mentioned in a recent report by Sturm.[24] It has been suggested instead that the fact that the observed barrier heights are higher that PtSi/Si could be due a lightly n-type SiGe layer, or in the surface of the SiGe layer, due to poor dopant control during growth. This would result in a surface-layer band-bending of the opposite type, raising the SiGe/Si offset barrier to observed values. While this is certainly possible, the effects of carrier energy losses in thick SiGe layers cannot be ignored, especially when energy losses in the much thinner PtSi films have been shown to have observable effects.[16] Models incorporating such n-type layers can perhaps explain some of the excess barrier height together with energy losses. However, the fitted energy-loss values are not unreasonable considering optical-phonon energies in Si and Ge (63 and 37 meV, respectively), optical-phonon scattering mean free paths (55 Å for holes in Si), and the distance travelled by the carriers (600-800 Å). The energy-loss picture by itself seems capable of explaining the observed data without invoking n-type layers.

Summary

The enhanced tunability of PtSi/SiGe/Si diodes should be understood as arising from two conceptually distinct, though related, mechanisms. The first mechanism is keeping the barrier height peak position fixed with increasing bias. The second mechanism is to shift the barrier height peak further away from the metal-semiconductor interface. It is the first mechanism that is key to achieving useful levels of tunability without decreasing quantum efficiency. Calculations show that the desired tunable cut-off range (5-12 µm) and voltage domain can be obtained with the same peak-to-metal distances ($\sim$ 60 Å) by using 20% Ge and doping levels of $\sim$ 4-8 x 10^{16} cm^{-3} throughout the depletion layer width ($\sim$ 4000 Å). The tunable range depends on known SiGe/Si offsets, but the value of the long-wavelength end of the range depends on the presently undetermined values of the intimate PtSi/SiGe barrier height, for which estimates were used. If the metal-to-peak thickness, or SiGe thickness, is large then the barrier height extrapolated by photoresponse must be interpreted taking into account the energy losses suffered by emitted carriers from semi-elastic collisions in the semiconductor. The predictions of this theoretical model are able to account for experimental data on a number of PtSi/SiGe/Si samples.

Acknowledgements

References

[1] For recent reviews, see M. Kimata and N. Tubouchi, in Infrared Photon Detectors, edited by A. Rogalski (SPIE Press, Bellingham 1995), and the articles in Physics of Thin Films Vol. 22, edited by M. Francombe (Academic Press, New York, to be published).

[2] P.W. Pellegrini, A. Golubovic, C.E. Ludington, and M.M. Weeks, Tech. Dig. Int. Electron. Device Mtg. 157 (1982).

[3] T.L. Lin, A. Ksendzov, S.M. Dejewski, E.W. Jones, R.W. Fathauer, T.N. Kraback, and J. Maserjian, IEEE Trans. Electron Devices 38, 1141 (1991).

[4] T.L. Lin, J.S. Park, T. George, E.W. Jones, R.W. Fathauer, and J. Maserjian, Appl. Phys. Lett. 61, 1122 (1992),

[5] J.R. Jimenez, J.C. Sturm, X. Xiao, and P.W. Pellegrini, Appl. Phys. Lett. 67, 506 (1995).

[6] I. Sagnes, C. Renard, and P. Badoz, J. Phys. IV, C6-139 (1994).

[7] A. G. U. Perera, H. X. Yuan, J.-W. Choe, and M.H. Francombe, Proc. SPIE 2475, 76 (1995).

[8] The asymptotic value is the value the Schottky barrier would have in the absence of image-force lowering, extrapolated from measurements of the actual Schottky barrier.

[9] S.M. Sze, Physics of Semiconductor Devices (Wiley, New York, 1981), Chapter 5.

[10] H. Kanaya, F. Hasegawa, E. Yamaka, T. Moriyama, and M. Nakayima, Jpn. J. Appl. Phys. 28, L544 (1989).

[11] H. K. Liou, X. Wu, U. Gennser, V.P. Kesan, S.S. Iyer, K.N. Tu, and E.S. Yang, Appl. Phys. Lett. 60, 577 (1992).

[12] X. Xiao, J.C. Sturm, S.R. Parihar, S. A. Lyon, D. Meyerhofer, S. Palfrey, and F.V. Shallcross, IEEE Electron Device Lett. EDL-14, 199 (1993).

[13] J.R. Jimenez and C. Chang, unpublished data.

[14] J.R. Jimenez, X. Xiao, J.C. Sturm, P.W. Pellegrini and M.M. Weeks, J. Appl. Phys. 75, 5160 (1994).

[15] J.R. Jimenez and Z. Atzmon, unpublished data.

[16] J.M. Mooney and J. Silverman, IEEE Trans. El. Dev. ED-32, 33 (1985).

[17] J.M. Mooney, J. Appl. Phys. 65 (7) 1989.

[18] C. A. Ventrice, Jr., V.P. LaBella, G. Ramaswamy, H.-P. Yu, and L.J. Schowalter, Phys. Rev. B 53 (1996) (in press).

[19] J.R. Jimenez, "Silicide/SiGe Diodes for Infrared Detection", Final Report (1993).

[20] J.R. Jimenez, X. Xiao, J.C. Sturm, P.W. Pellegrini and M.M. Weeks, SPIE Proc 2225, 393 (1994).

[21] J.R. Jimenez, X. Xiao, J.C. Sturm, P.W. Pellegrini, and M. Chi, Mater. Res. Soc. Symp. Proc. 320, 293 (1994).

[22] J. Bean, Proc. IEEE 80, 571 (1992).

[23] R.T. Tung, Phys. Rev. B 45, 13509 (1992).

[24] J.C. Sturm, "$Si_{1-x}Ge_x$/Si Heterostructures for Infrared Detectors", Final Report, Contract F19628-93-K-0013 (1995).
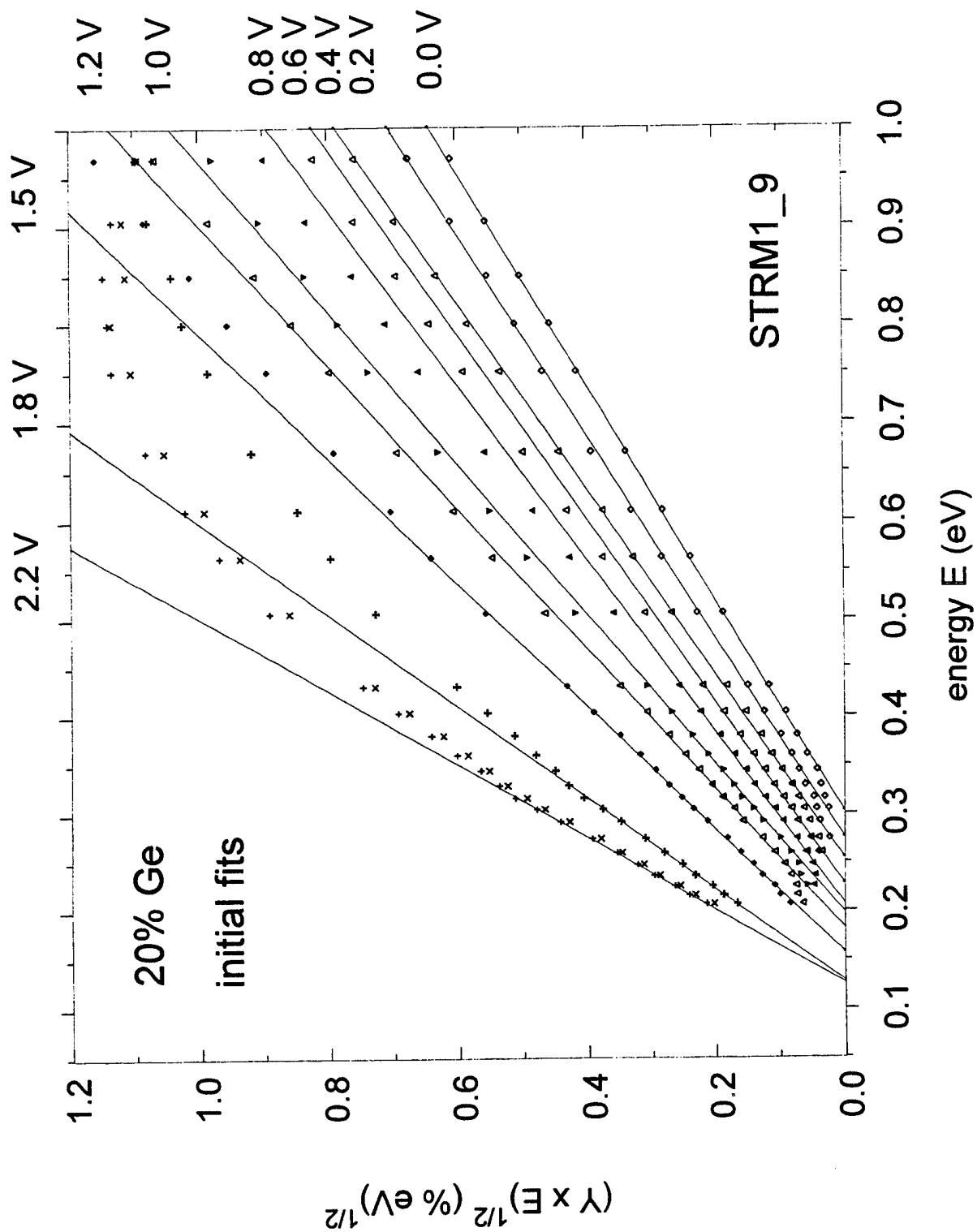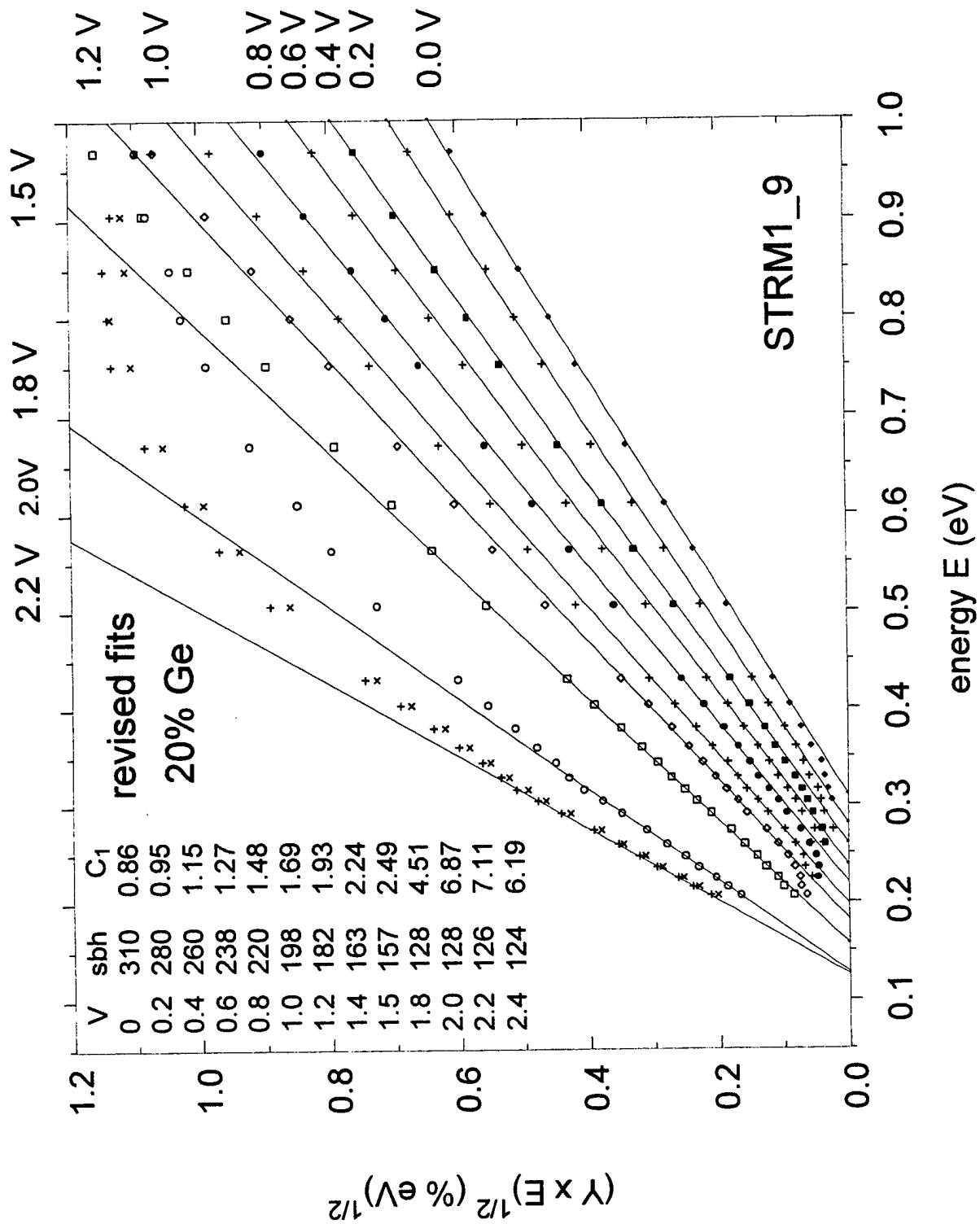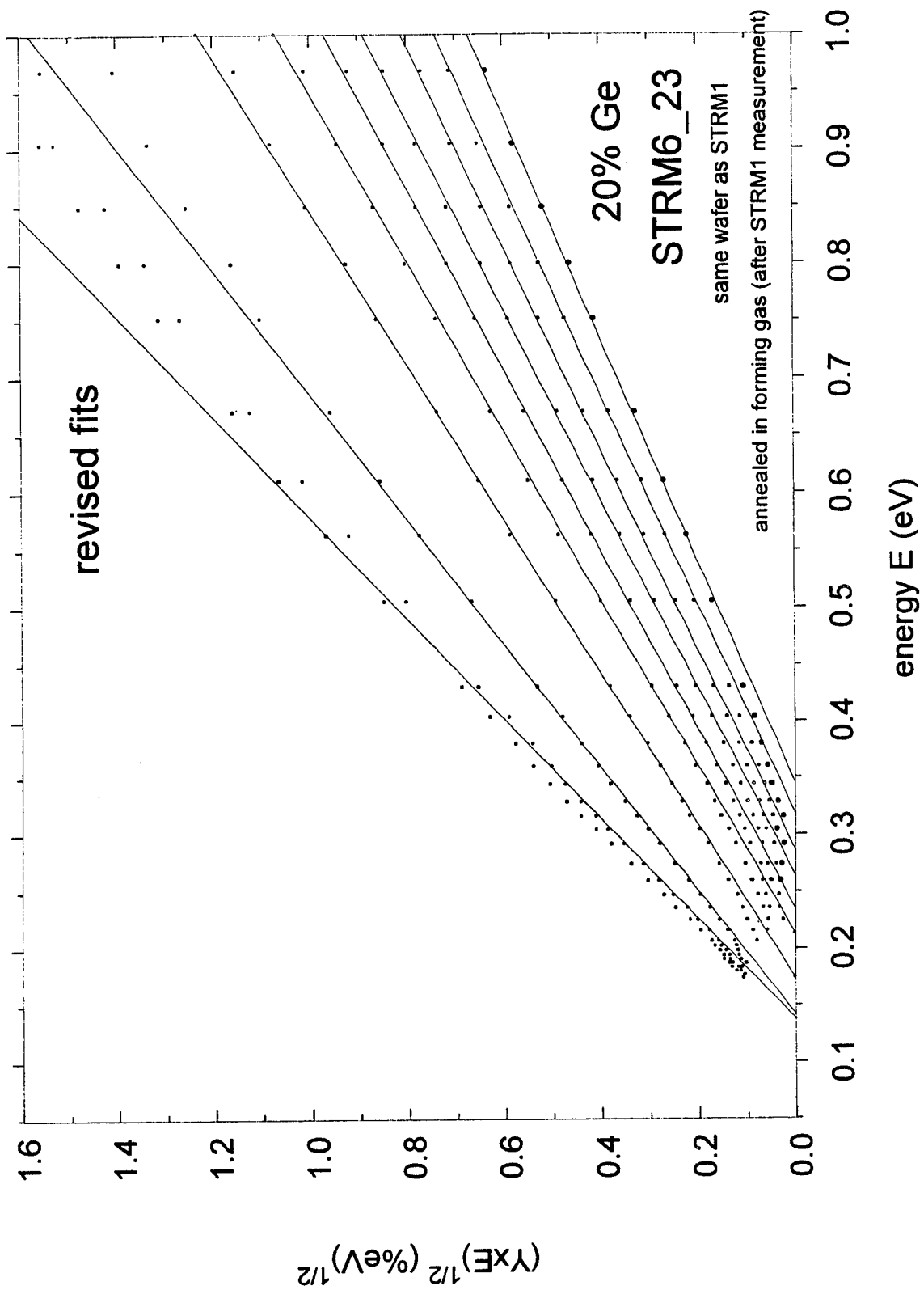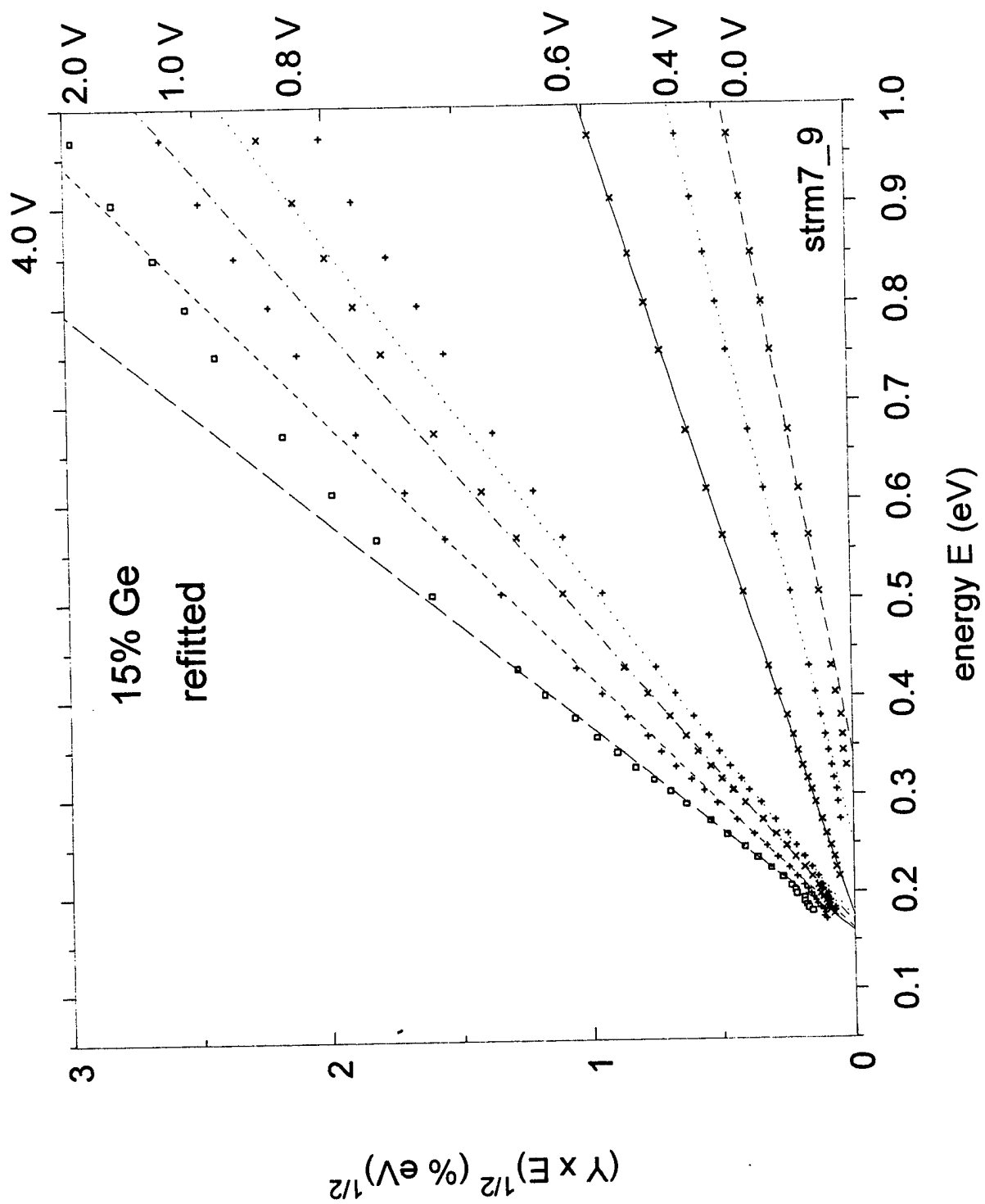
Figure 18

revised fits
20% Ge

2.2 V   2.0v   1.8 V   1.5 V

1.2 V
1.0 V
0.8 V
0.6 V
0.4 V
0.2 V
0.0 V

STRM1_9

V	sbh	C_1
0	310	0.86
0.2	280	0.95
0.4	260	1.15
0.6	238	1.27
0.8	220	1.48
1.0	198	1.69
1.2	182	1.93
1.4	163	2.24
1.5	157	2.49
1.8	128	4.51
2.0	128	6.87
2.2	126	7.11
2.4	124	6.19

energy E (eV)

$(Y \times E)^{1/2}$ (% eV)$^{1/2}$

Figure 19

19

Figure 20

20

Figure 21

Figure 22

Figure 23

PtSi/SiGe/Si 5% Ge

original fits

bias	C_1	SBH
0.2V	0.8	223
0.5V	1.6	213
1V	3.8	198
2V	10.7	187
3V	15.0	182
4V	16.8	179
8V	17.7	169

8 V
4 V
3 V

2 V

1 V

0.5 V

0.2 V

strm9_9

energy E (eV)

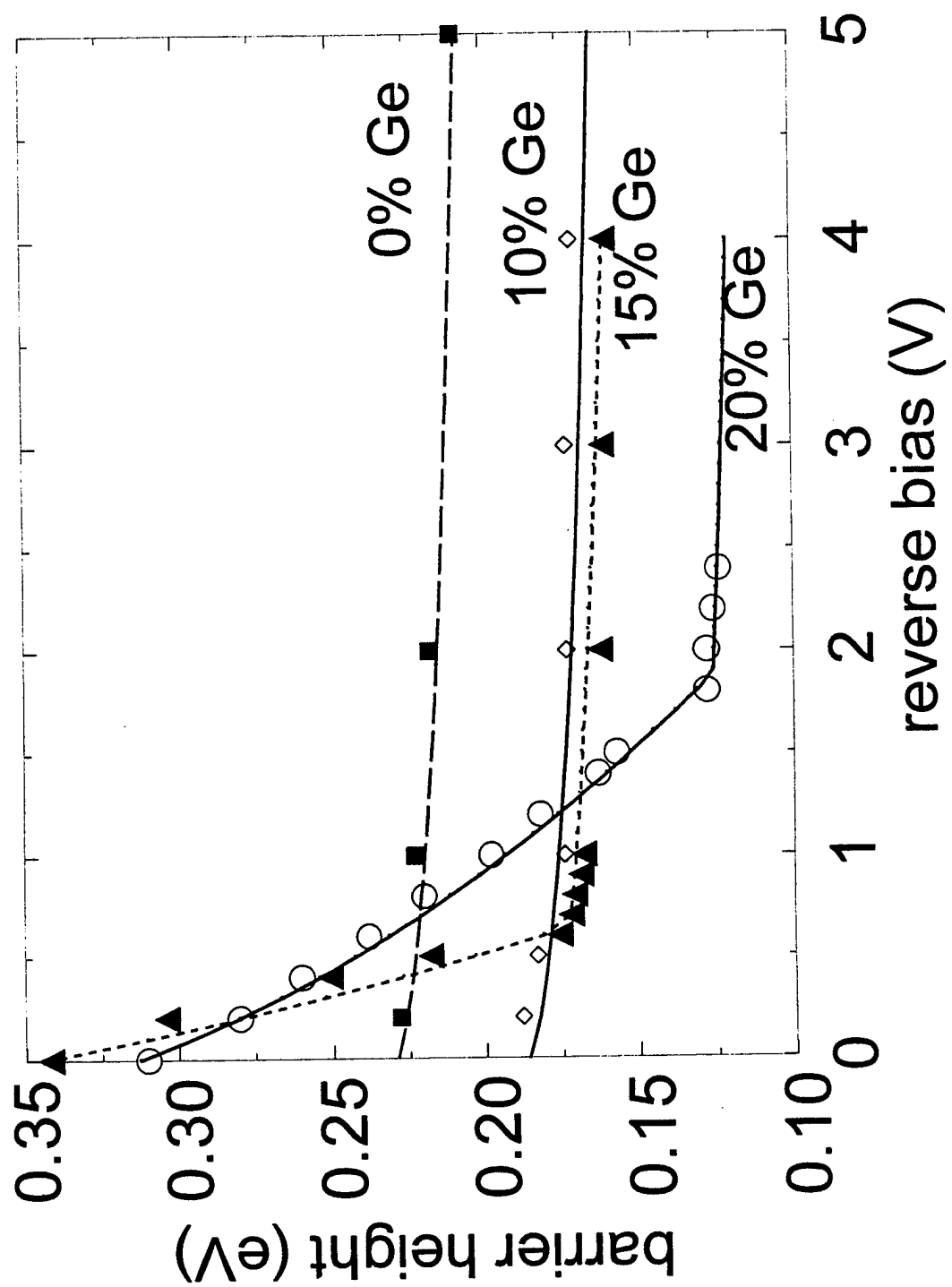$(Y \times E)^{1/2}$ (% x eV)$^{1/2}$
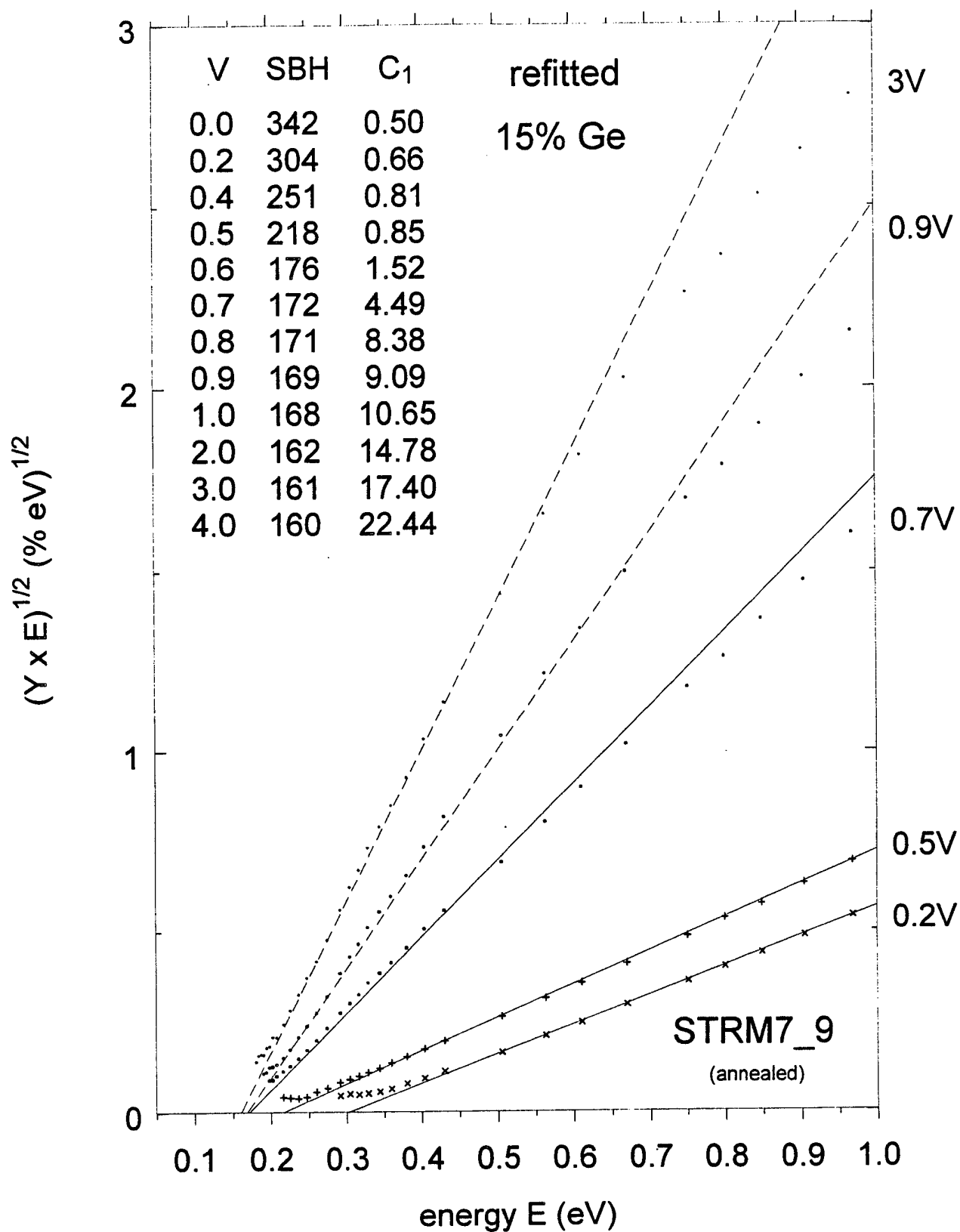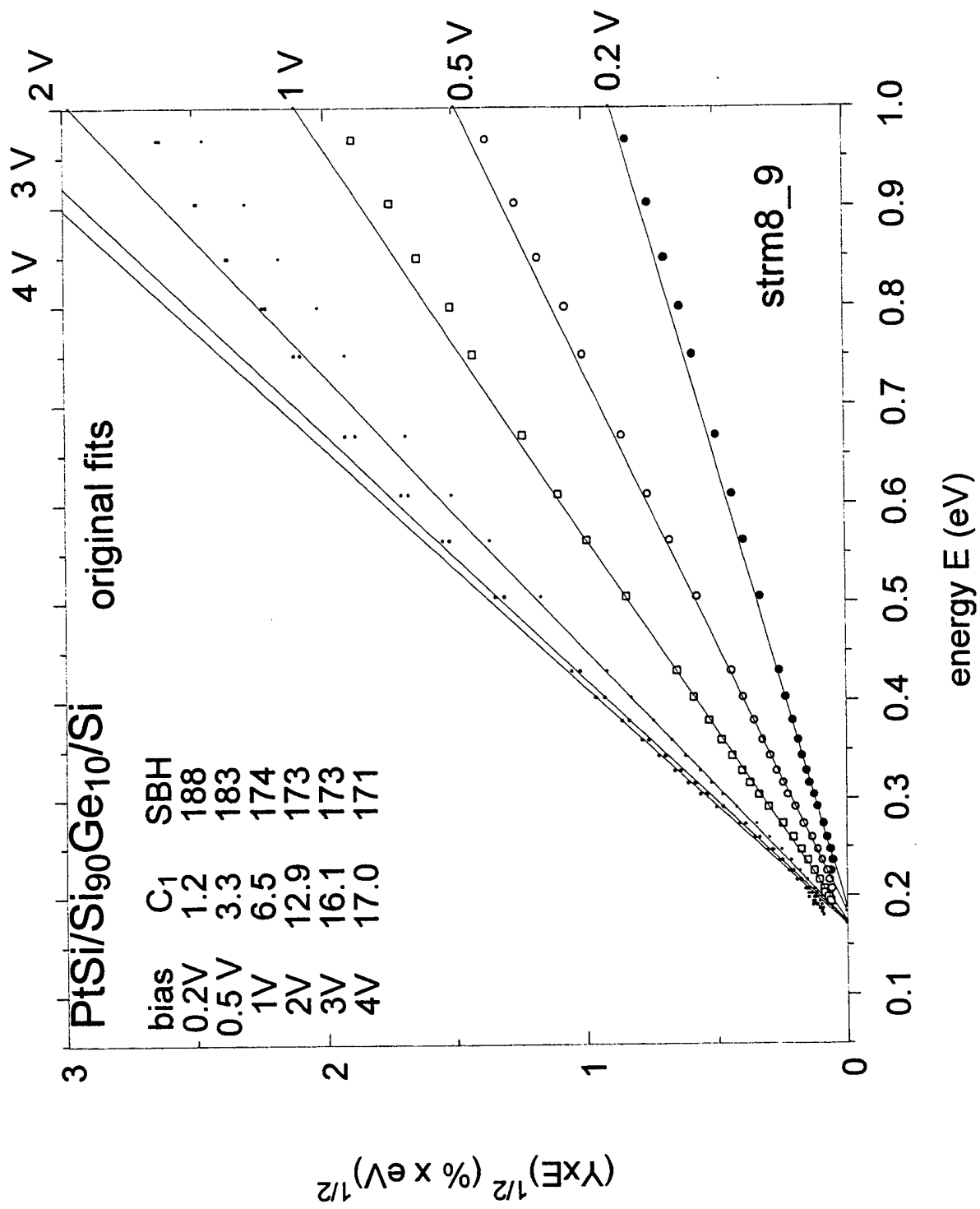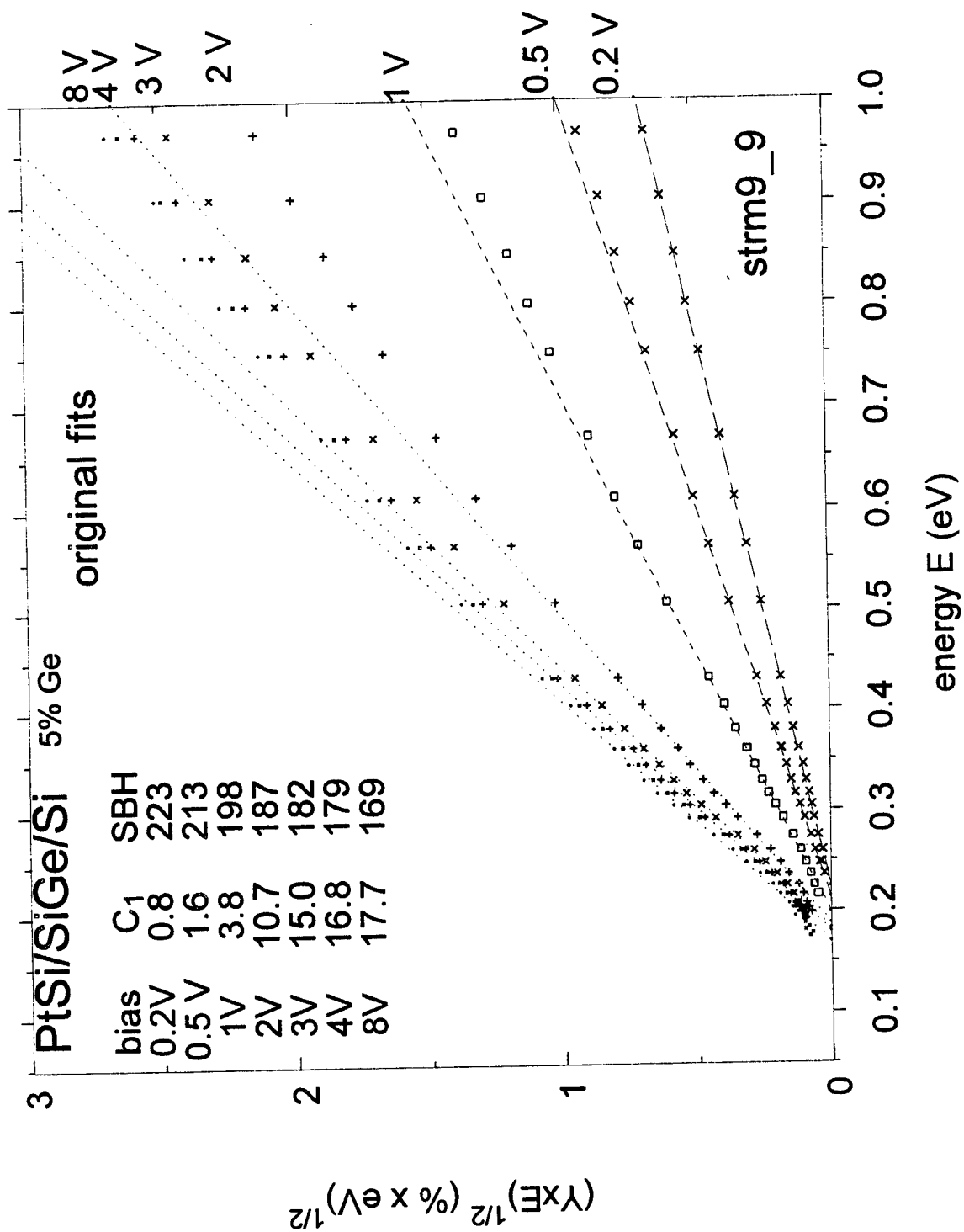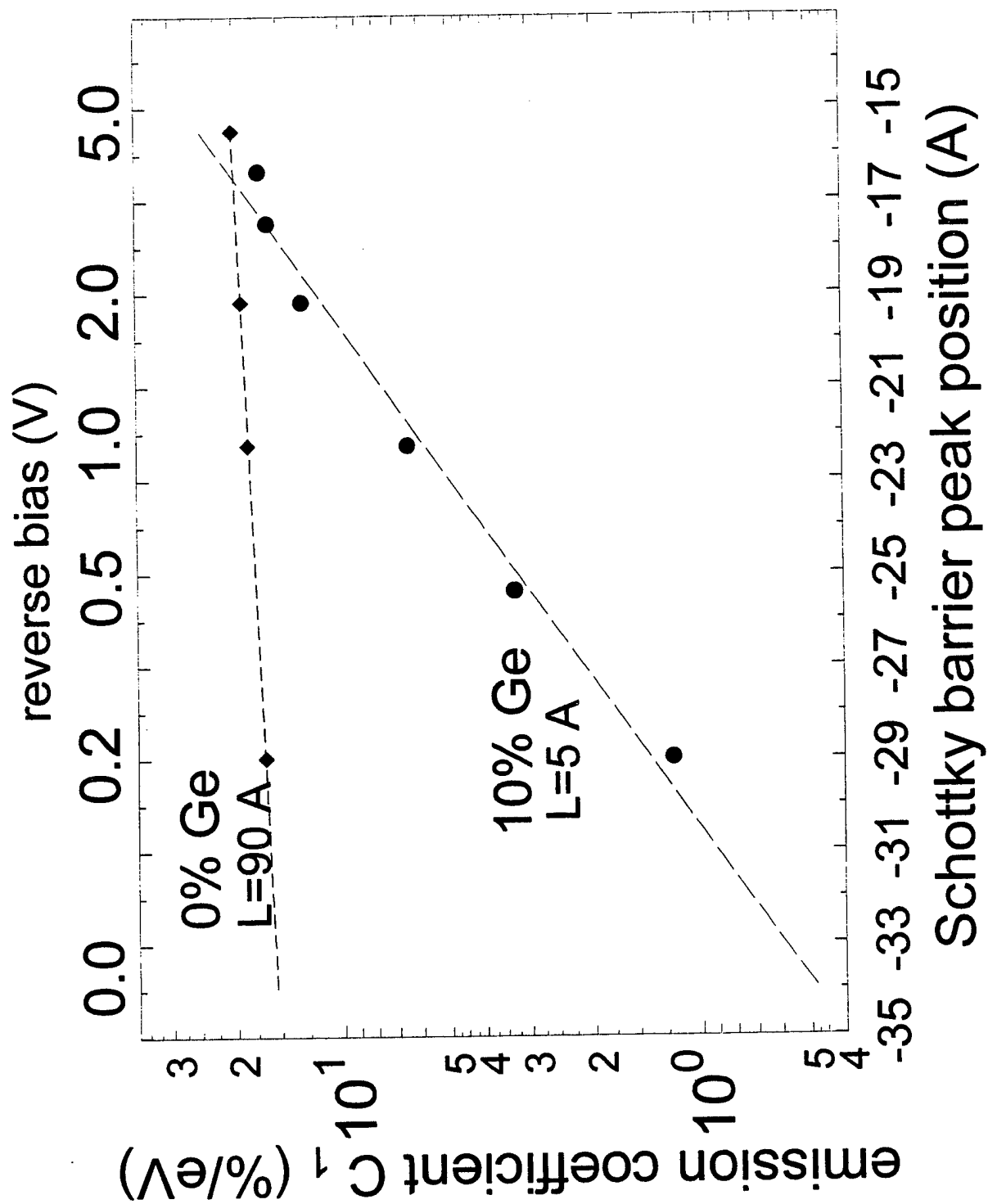
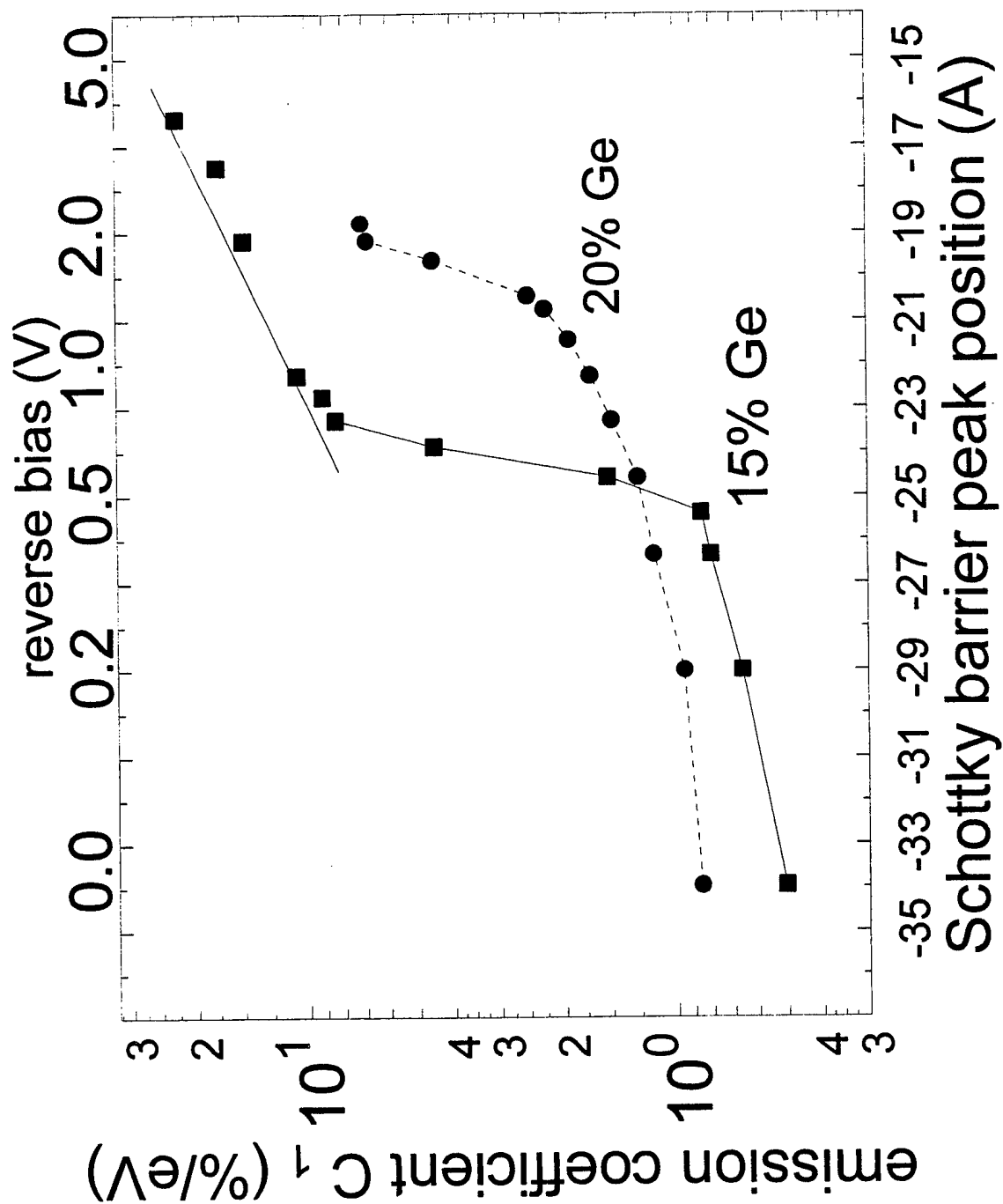**Figure 24**

24

Figure 25

Figure 28

Figure 29

MISSION

OF

ROME LABORATORY

Mission. The mission of Rome Laboratory is to advance the science and technologies of command, control, communications and intelligence and to transition them into systems to meet customer needs. To achieve this, Rome Lab:

a. Conducts vigorous research, development and test programs in all applicable technologies;

b. Transitions technology to current and future systems to improve operational capability, readiness, and supportability;

c. Provides a full range of technical support to Air Force Materiel Command product centers and other Air Force organizations;

d. Promotes transfer of technology to the private sector;

e. Maintains leading edge technological expertise in the areas of surveillance, communications, command and control, intelligence, reliability science, electro-magnetic technology, photonics, signal processing, and computational science.

The thrust areas of technical competence include: Surveillance, Communications, Command and Control, Intelligence, Signal Processing, Computer Science and Technology, Electromagnetic Technology, Photonics and Reliability Sciences.